

**Spectral aerosol  
optical properties by  
a multi-instrumental  
approach**

S. Segura et al.

# Determination and analysis of spectral aerosol optical properties by a multi-instrumental approach

S. Segura<sup>1</sup>, V. Estellés<sup>1</sup>, G. Titos<sup>2</sup>, H. Lyamani<sup>2</sup>, M. P. Utrillas<sup>1</sup>, P. Zotter<sup>3</sup>,  
A. S. H. Prévôt<sup>3</sup>, G. Močnik<sup>4</sup>, L. Alados-Arboledas<sup>2</sup>, and J. A. Martínez-Lozano<sup>1</sup>

<sup>1</sup>Departament de Física de la Terra i Termodinàmica, Universitat de València, Burjassot (Valencia), Spain

<sup>2</sup>Centro Andaluz de Medio Ambiente, Junta de Andalucía and Universidad de Granada, Granada, Spain

<sup>3</sup>Laboratory Atmospheric Chemistry (LAC), Paul Scherrer Institute, Villigen, Switzerland

<sup>4</sup>Aerosol d. o. o., Research and Development Department, Ljubljana, Slovenia

Received: 19 December 2013 – Accepted: 9 February 2014 – Published: 26 February 2014

Correspondence to: S. Segura (sara.segura@uv.es)

Published by Copernicus Publications on behalf of the European Geosciences Union.

Title Page

Abstract

Introduction

Conclusions

References

Tables

Figures

⏪

⏩

◀

▶

Back

Close

Full Screen / Esc

Printer-friendly Version

Interactive Discussion

## Abstract

Continuous in-situ measurements of aerosol optical properties were conducted from 20 June to 20 July in Granada (Spain) with a 7-wavelength Aethalometer, a Multi Angle Absorption Photometer, and a 3-wavelength integrating Nephelometer. The aim of this work is to describe a methodology to obtain the absorption coefficients ( $b_{\text{abs}}$ ) for the different Aethalometer wavelengths. In this way, data have been compensated using algorithms which best estimate the compensation factors needed. Two empirical factors are used to infer the absorption coefficients from the Aethalometer measurements:  $C$  – the parameter describing the enhancement of absorption by particles in the filter matrix due to multiple scattering of light in the filter matrix; and  $f$  – the parameter compensating for non-linear loading effects in the filter matrix. Spectral dependence of  $f$  found in this study is not very strong. Values for the campaign lie in the range from 1.15 at 370 nm to 1.11 at 950 nm. Wavelength dependence in  $C$  proves to be more important, and also more difficult to calculate. The values obtained span from 3.40 at 370 nm to 4.35 at 950 nm. Furthermore, the temporal evolution of the Ångström exponent of absorption ( $\alpha_{\text{abs}}$ ) and the single scattering albedo ( $\omega_0$ ), is presented. On average  $\alpha_{\text{abs}}$  is around  $1.1 \pm 0.3$ , and  $\omega_0$  is  $0.78 \pm 0.08$  and  $0.74 \pm 0.09$  at 370 and 950 nm, respectively. These are typical values for sites with a predominance of absorbing particles, and the urban measurement site in this study is such. The  $b_{\text{abs}}$  average values are of  $16 \pm 10 \text{ Mm}^{-1}$  (at 370 nm) and  $5 \pm 3 \text{ Mm}^{-1}$  (at 950 nm), respectively. Finally, differences between working days and Sunday have been further analyzed, obtaining higher  $b_{\text{abs}}$  and lower  $\omega_0$  during week than on Sundays as a consequence of the influence of diesel traffic.

## 1 Introduction

The radiative forcing in the Earth's atmosphere caused by aerosols is highly uncertain (IPCC, 2013). The direct effect of aerosol influence is exhibited by scattering and/or

AMTD

7, 1871–1916, 2014

### Spectral aerosol optical properties by a multi-instrumental approach

S. Segura et al.

Title Page

Abstract

Introduction

Conclusions

References

Tables

Figures

⏪

⏩

◀

▶

Back

Close

Full Screen / Esc

Printer-friendly Version

Interactive Discussion





Weingartner et al., 2003; Arnott et al., 2005; Schmid et al., 2006), and have proven to give quite satisfactory results when compared to other non-filter based instruments.

From the instruments mentioned above, the MAAP is the newest filter-based instrument for measuring the aerosol absorption coefficient (Petzold and Schönlinner, 2004; Petzold et al., 2005). Measurements provided by the MAAP are only available for one wavelength, which is a disadvantage since it is important to determine both  $b_{\text{abs}}$  and its spectral dependence. This information can be obtained by combining the MAAP measurements with those performed by a multi-wavelength Aethalometer AE-31, which performs measurements at 7 different channels covering the range from the UV (370 nm) to NIR (950 nm).

The aim of this work is to obtain the spectral variation of the compensation factors of the Aethalometer data and then apply them to the measurements performed at the different channels of the Aethalometer. In this way, the aerosol absorption coefficients at all the different Aethalometer channels are calculated and then, other optical parameters, such as the spectral single scattering albedo ( $\omega_0$ ) or the Ångström exponent of absorption ( $\alpha_{\text{abs}}$ ), are determined and analyzed.

The data set presented in this study was measured during one month, from 29 June 2012 to 29 July 2012, in Granada (Spain) using a MAAP, an Aethalometer, and a Nephelometer. In this work we will discuss the methodology used for compensating the Aethalometer and MAAP data. Finally, the temporal evolution of the results obtained is presented and compared with results in other works to evaluate the reliability of the data.

## 2 Site description and instrumentation

### 2.1 Measurement site

Measurements presented in this study were performed in Granada, from 29 June to 29 July 2012. Granada (37.18° N, 3.58° W, 680 m.a.s.l.) is a non-industrialized

## Spectral aerosol optical properties by a multi-instrumental approach

S. Segura et al.

Title Page

Abstract

Introduction

Conclusions

References

Tables

Figures

⏪

⏩

◀

▶

Back

Close

Full Screen / Esc

Printer-friendly Version

Interactive Discussion



medium-size city located in southeastern Spain with a population of around 500 000 inhabitants considering the whole metropolitan area (<http://www.juntadeandalucia.es/>). Near continental conditions prevail at this site and are responsible for large temperature differences, providing cool winters and hot summers (Lyamani et al., 2010).

The measurement station is located in the southern part of the city, less than 500 m away from a highway that surrounds the city. Local aerosol sources are mainly road traffic (dominated by diesel engines) together with soil re-suspension, especially during the warm-dry season when the reduced rainfall may increase the contribution of local mineral dust. Due to its location in the Mediterranean basin, it is influenced by two major aerosol source regions: Europe, as a source of anthropogenic pollutants, and North Africa as a source of natural mineral dust (Lyamani et al., 2010).

## 2.2 Instrumentation

Sampling for all the different instruments was obtained using a stainless steel tube with 20 cm diameter and 5 m length (Lyamany et al., 2008). The inlet was located about 15 m above the ground. Measurements were carried out without an aerosol size cut-off or heating of the sampled air. From the tube, several stainless steel pipes led the sampled air to each instrument at the appropriate flows. Different diameters were adjusted to maintain the laminar flow in the tubes and minimize particle losses (Baron and Willeke, 2005).

The aerosol light absorption coefficient was measured using two different filter-based instruments. The MAAP (Thermo Scientific) measures the light transmitted through and backscattered from a particle-loaded filter. The  $b_{\text{abs, MAAP}}$  at 637 nm (Müller et al., 2011) is calculated using radiative transfer model which includes a treatment of the scattering effects of the filter matrix and the light scattered by the aerosol component. A detailed description of the method is provided by Petzold and Schönlinner (2004). The MAAP works at a constant flow rate of  $16.7 \text{ L min}^{-1}$  and provides measurements every minute. The total method uncertainty for the aerosol light absorption coefficient inferred from

## Spectral aerosol optical properties by a multi-instrumental approach

S. Segura et al.

Title Page

Abstract

Introduction

Conclusions

References

Tables

Figures

◀

▶

◀

▶

Back

Close

Full Screen / Esc

Printer-friendly Version

Interactive Discussion

MAAP measurement is around 12 % (Petzold and Schönlinner 2004; Petzold et al., 2005).

The MAAP was believed to be the instrument which is the least affected by artifacts for obtaining the aerosol absorption coefficient among all the different filter-based methods. Different studies showed that  $b_{\text{abs, MAAP}}$  measured by MAAP is in good agreement with those measured by photoacoustic spectrometry (e.g. Petzold et al., 2005; Sheridan et al., 2005). However, a recent study by Hyvärinen et al. (2013) showed that MAAP measurements suffer from some artifacts in locations with high concentrations of light absorbing particles. Therefore, to avoid these artifacts, MAAP data have been compensated using the method described in Hyvärinen et al. (2013). A more detailed explanation can be found in Sect. 3.1.

The other instrument used to measure the  $b_{\text{abs}}$  is an Aethalometer model AE-31-ER (Magee Scientific). The AE-31 measures light attenuation at 7 different wavelengths covering the UV (370 nm), visible (470, 520, 590, and 660 nm), and NIR (880 nm and 950 nm) ranges. A complete description of the operating principles of Aethalometers can be found in Hansen et al. (2005).

The Aethalometer measures the light attenuation through a quartz filter matrix as aerosols are deposited on the filter. This parameter is defined by:

$$\text{ATN}(\lambda) = -\ln\left(\frac{I(\lambda)}{I_0(\lambda)}\right) \quad (1)$$

where  $I$  is the intensity of light that passes through the loaded filter, and  $I_0$  is the intensity of light passing through the unloaded part of the filter. The attenuation coefficient at each wavelength,  $b_{\text{ATN}}(\lambda)$  can be obtained by:

$$b_{\text{ATN}}(\lambda) = \frac{A}{V} \frac{\Delta \text{ATN}(\lambda)}{\Delta t} \quad (2)$$

where  $A$  is the filter spot area (1.67 cm<sup>2</sup>),  $V$  the volumetric flow rate, and  $\Delta \text{ATN}$  is the variation in the attenuation measured during the time interval ( $\Delta t$ ). The attenuation

## Spectral aerosol optical properties by a multi-instrumental approach

S. Segura et al.

Title Page

Abstract

Introduction

Conclusions

References

Tables

Figures

◀

▶

◀

▶

Back

Close

Full Screen / Esc

Printer-friendly Version

Interactive Discussion







following equation (Petzold et al., 2005):

$$b_{\text{atn, MAAP}} = 0.5 \frac{A}{V} \ln \left( \frac{R_0}{R} \right) \quad (3)$$

where, in our case,  $(R_0/R)$  is the ratio of the photodetector signal at  $165^\circ$  for a particle free and a particle loaded filter, respectively. The multiplication factor of 0.5 in Eq. (3) has to be applied because the light passes through the layer of sampled aerosol twice before reaching the photodetector.

The value obtained from Eq. (3) does not correspond to the absorption coefficient since there is a filter loading effect which influences the measured signals. Petzold et al. (2005) determined an empirical method to compensate this artifact using test aerosols. These test aerosols consisted of pure black aerosol samples from kerosene flame particles, and externally mixed grey and black aerosols of varying single scattering albedo. The obtained relation for the aerosol absorption coefficient for these aerosols using the reflected signal is:

$$b_{\text{abs, MAAP}} = b_{\text{atn, MAAP}} \left( 0.226 + 1.415 \frac{R}{R_0} \right)^{-1} \quad (4)$$

Similar to Hyvärinen et al. (2013) values automatically provided by the MAAP ( $b_{\text{atn, MAAP}}$ ) are lower than those calculated from raw reflected signal for high absorption coefficients (Fig. 1). We do not observe any systematic saturation in the measurements as found previously (Kanaya et al., 2008) or large discontinuities in the data at the tape advance (Brito et al., 2013). This indicates that the use of the reflection signals rather than the default values compensated the data successfully. To check the compensation, we plot (Fig. 2a and b) the average value of the MAAP attenuation and absorption coefficient in a spot loading bin (with width  $0.3 \mu\text{g cm}^{-2}$ ) as a function of the loading of the spot with BC between a clean filter (no loading) and the BC value with enough data in the campaign to gather enough statistics (just above  $5 \mu\text{g cm}^{-2}$ ). The slope of the compensated MAAP absorption coefficient is half of that of the uncompensated ones,

**Spectral aerosol optical properties by a multi-instrumental approach**

S. Segura et al.

Title Page

Abstract

Introduction

Conclusions

References

Tables

Figures

◀

▶

◀

▶

Back

Close

Full Screen / Esc

Printer-friendly Version

Interactive Discussion





where  $m = 5 \text{ ng}$ ,  $\sigma_{\text{ATN}}(\lambda)$  is the mass-specific attenuation cross-section in  $\text{m}^2 \text{g}^{-1}$ ,  $\Delta t$  is the time based period (set to 5 min in our case), and  $Q$  is the sampling flow in  $\text{L min}^{-1}$  ( $4 \text{ L min}^{-1}$  in our instrument). The attenuation cross section is calculated using the following equation:

$$\alpha_{\text{ATN}} = \frac{14625}{\lambda [\text{nm}]} \quad (6)$$

This equation is based on a calibration at 880 nm using the Malissa–Novakov method, a solvent based thermal desorption method for elemental carbon analysis (Gundel et al., 1984).

Also, as a consequence of random voltage fluctuations and from recording discontinuities which take place during the Aethalometer's tape advance a third criterion related to the upper detection limit is applied (deCastro et al., 2008). To identify these bad quality data, the 99th percentile of the attenuation coefficient (i.e.,  $162.2 \text{ Mm}^{-1}$  at 660 nm) was chosen as the extreme upper limit.

From the whole data set, 4% of the data did not satisfy any of these three criteria, leaving a total number of 8276 of attenuation measurements.

### 3.2.2 Data compensation

Aethalometer artifacts, unlike MAAP, are well known and five different algorithms have been proposed to correct them (Weingartner et al., 2003; Arnott et al., 2005; Schmid et al., 2006; Virkkula et al., 2007; Collaud-Coen et al., 2010). The beam crossing the filter suffers: (1) multi-scattering effects due to the filter fibers, (2) single scattering effects, due to the aerosol particles deposited in the filter, and (3) filter loading effects, which are related to the shadowing produced as the particles accumulate on the filter. The result of these optical interactions is the  $b_{\text{ATN}}$  is generally larger than  $b_{\text{abs}}$  (Petzold et al., 1997; Ballach et al., 2001).

Due to the aforementioned aerosol-filter interactions, the Aethalometer requires specific site compensation factors. In this sense, we have calculated this compensation

## Spectral aerosol optical properties by a multi-instrumental approach

S. Segura et al.

Title Page

Abstract

Introduction

Conclusions

References

Tables

Figures

⏪

⏩

◀

▶

Back

Close

Full Screen / Esc

Printer-friendly Version

Interactive Discussion



## Spectral aerosol optical properties by a multi-instrumental approach

S. Segura et al.

Title Page

Abstract

Introduction

Conclusions

References

Tables

Figures

⏪

⏩

◀

▶

Back

Close

Full Screen / Esc

Printer-friendly Version

Interactive Discussion

factors for our site and used them to compensate the Aethalometer data by applying the algorithms proposed by Weingartner et al. (2003) and Schmid et al. (2006). The reason to select these two algorithms out of the five existing ones is that Weingartner et al. (2003) and Schmid et al. (2006) found a way to obtain the spectral dependence of the multiple scattering compensation factor from aerosol single scattering albedo. Knowing this spectral dependence will allow us to convert  $b_{\text{ATN}}$  to  $b_{\text{abs}}$  for all 7 Aethalometer wavelengths. The most important difference between these two algorithms lies in the fact that Weingartner's algorithm does not consider the artifact produced by the single scattering effect, while Schmid's does.

In their test with ammonium sulfate, Weingartner et al. (2003) found no significant dependence of  $b_{\text{ATN}}$  on the scattering component of the aerosol in the filter. Therefore, they proposed an algorithm to obtain  $b_{\text{abs}}$  without taking into account the single scattering effect of the aerosols:

$$b_{\text{abs}} = \frac{b_{\text{ATN}}}{C \cdot R(f, \text{ATN})} \quad (7)$$

where  $C$  compensates for the multiple scattering effects exhibiting values  $\geq 1$ , and  $R(f, \text{ATN})$  for the loading-effect with values  $\leq 1$ , respectively. The loading compensation depends on the amount of the sample collected on the filter and is hence dependent on the attenuation measured by the Aethalometer. The parameter can be expressed as proposed in Weingartner et al. (2003):

$$R(f, \text{ATN}) = \left( \frac{1}{f} - 1 \right) \frac{\ln \text{ATN} - \ln 10\%}{\ln 50\% - \ln 10\%} + 1 \quad (8)$$

where  $f$  is the shadowing factor, which depends on the type of the aerosols. This parameter has been calculated by minimizing the difference between the ratio of  $b_{\text{ATN}}$  before and after the filter spot change. The calculated median  $f$  values were plotted as a function of  $\lambda$  and fitted with a linear equation (Sandradewi et al., 2008b). Values obtained for this parameter are shown in Table 1.

## Spectral aerosol optical properties by a multi-instrumental approach

S. Segura et al.

Title Page

Abstract

Introduction

Conclusions

References

Tables

Figures

⏪

⏩

◀

▶

Back

Close

Full Screen / Esc

Printer-friendly Version

Interactive Discussion



The effect of the compensation of the Aethalometer measurements is shown in Fig. 2c and d. The slope reduces significantly to a value which is non-distinguishable from 0 – the compensation is efficient in eliminating the loading effects. The difference between the intersect  $7.14 \text{ Mm}^{-1}$  and the campaign average  $7.10 \text{ Mm}^{-1}$  satisfies the empirical 5% criterion. Additionally, the value lies extremely close to the average and the intersect determined from the analysis of the MAAP compensation (Sect. 3.1).

Since the loading effect is small for lightly loaded filters (Weingartner et al., 2003),  $C$  can be determined by comparing low loaded Aethalometer measurements ( $\text{ATN} < 10\%$ ) with the ones obtained by a different comparison instrument. In this study we chose the MAAP ( $b_{\text{abs, MAAP}}$ ) as a comparison and  $C$  is determined using the equation proposed in Weingartner et al. (2003) as:

$$C = \frac{b_{\text{ATN}}(\text{ATN} < 10)}{b_{\text{abs, MAAP}}} \quad (9)$$

$C$  has been calculated at 637 nm, as the MAAP measurements are performed at this wavelength. Since the nearest wavelengths in the Aethalometer are 590 and 660 nm,  $b_{\text{ATN}}$  (637 nm) has been calculated by approximating the wavelength dependence of the attenuation spectra for each measurement to a power-law expression, such as:

$$b_{\text{ATN}}(\lambda) = a \cdot \lambda^{-\alpha_{\text{atn}}} \quad (10)$$

where  $a$  is a fitting parameter and  $\alpha_{\text{atn}}$  is the Ångström exponent of attenuation.

After taking logarithm of Eq. (10), a “linear fit” was applied to the log-log curve:

$$\ln[b_{\text{ATN}}(\lambda)] = \ln a - \alpha_{\text{atn}} \ln(\lambda) \quad (11)$$

To calculate  $C$ ,  $b_{\text{ATN}}$  at 637 nm for the Aethalometer data has to be calculated since  $b_{\text{abs, MAAP}}$  in Eq. (9) is related to 637 nm. The average  $C$  value at the wavelength of 637 nm was determined to be  $C_{637} = 4.22 \pm 0.06$  from the arithmetic mean (95% confidence level of the mean) of the ratios of  $b_{\text{ATN}}$  (637) and  $b_{\text{abs, MAAP}}$  (Schmid et al.,

## Spectral aerosol optical properties by a multi-instrumental approach

S. Segura et al.

Title Page

Abstract

Introduction

Conclusions

References

Tables

Figures

⏪

⏩

◀

▶

Back

Close

Full Screen / Esc

Printer-friendly Version

Interactive Discussion



2006). Collaud-Coen et al. (2010) obtained different  $C$  values ranging between 2.8 and 7.8 at several sites. In particular, from the different sites chosen in that paper, our value is close to those obtained ( $C_{660} = 4.12 \pm 0.06$ ) at Cabauw (the Netherlands), a background site located near populated and industrialized areas (Collaud-Coen et al., 2010).

Some publications (Lack et al., 2009; Nakayama et al., 2010) indicate that the multiple scattering compensation factor might depend on the particle size, as the aerosol penetration depth into the filter varies depending on the size. Since this effect is still difficult to quantify (Rizzo et al., 2011), it is not straightforward to conclude if there will be an overestimation or underestimation in our absorption coefficients due to this effect. A significant part of the aerosol load on the filter tape on the measurement site is always diesel exhaust particles, so at least this part of the loading is extremely homogeneous. Therefore, we did not consider this effect further in this manuscript.

### 3.2.3 Spectral dependence of $C$ and aethalometer absorption coefficients

Schmid et al. (2006) parameterized (based on Arnott et al., 2005) the spectral dependence of  $C$  using the following expression:

$$C(\lambda) = C^*(\lambda) + m_s(\lambda) \frac{\omega_0(\lambda)}{1 - \omega_0(\lambda)} \quad (12)$$

where  $C^*$  is the multiple scattering compensation factor which includes the effects of aerosol scattering,  $m_s$  is the fraction of the aerosol scattering coefficient erroneously interpreted as absorption,  $\omega_0$  is the aerosol single scattering albedo, and  $\lambda$  is the wavelength. Both  $C^*(\lambda)$  and  $m_s$  were calculated for ammonium sulfate particles by Arnott et al. (2005). They however showed that these values gave unsatisfactory results when used to correct ambient measurements.

Equation (12) has been used to obtain  $C_{637}^*$  using  $C_{637}$  calculated in the previous section with Eq. (9). Once it is calculated,  $C^*$  values for the other wavelengths will be obtained assuming the same wavelength dependence as in Arnott et al. (2005).

Values of  $m_s$  used here were taken from Arnott et al. (2005) since with our data it is not possible to determine them.  $\omega_0(637)$  was calculated using the following expression (Schmid et al., 2006):

$$\omega_0(637) = \frac{b_{\text{scat}}(637)}{b_{\text{scat}}(637) + b_{\text{abs, MAAP}}(637)} \quad (13)$$

where  $b_{\text{abs, MAAP}}$  is the MAAP absorption coefficient measured at 637 nm and  $b_{\text{scat}}$  is the scattering coefficient from the Nephelometer, interpolated to 637 nm by using Eqs. (10) and (11) for  $b_{\text{scat}}(\lambda)$ .

To obtain the different  $C$  values for the remaining Aethalometer wavelengths,  $\omega_0(\lambda)$ ,  $C^*(\lambda)$ , and  $m_s(\lambda)$ , are required (Eq. 12). Equation (13) is not useful in this case since MAAP absorption is only obtained at one wavelength and cannot be applied for the other Aethalometer channels. Therefore, for calculating  $\omega_0(\lambda)$  we used the following expression (Schmid et al., 2006):

$$\omega_0(\lambda) = \frac{\omega_{0,\text{ref}} \left( \frac{\lambda}{\lambda_{\text{ref}}} \right)^{-\alpha_{\text{scat}}}}{\omega_{0,\text{ref}} \left( \frac{\lambda}{\lambda_{\text{ref}}} \right)^{-\alpha_{\text{scat}}} + (1 - \omega_{0,\text{ref}}) \left( \frac{\lambda}{\lambda_{\text{ref}}} \right)^{-\alpha_{\text{abs}}}} \quad (14)$$

where  $\omega_{0,\text{ref}}$  is the reference single scattering albedo calculated at 637 nm ( $\lambda_{\text{ref}}$ ) using Eq. (13),  $\alpha_{\text{scat}}$  is the Ångström exponent of scattering and  $\alpha_{\text{abs}}$  is the Ångström exponent of absorption.  $\alpha_{\text{scat}}$  depends on the  $b_{\text{scat}}$  measured at different wavelengths and can be obtained from the nephelometer measurements (450–700 nm). However,  $\alpha_{\text{abs}}$  is calculated from the  $b_{\text{abs}}$  measured by the Aethalometer at different wavelengths.

Schmid et al. (2006) used fixed values for  $\alpha_{\text{scat},450-700}$  and  $\omega_0(545)$  measurements given by Chand et al. (2006) for the Amazonia, and a range of different  $\alpha_{\text{abs}}$  based on Kirchstetter et al. (2004) to obtain a parameterization function of  $C(\lambda)$  and  $\alpha_{\text{abs}}$ . Then they applied an iterative procedure over this function to obtain  $C(\lambda)$  and  $\alpha_{\text{abs}}$ . The fixed values used were  $\alpha_{\text{scat}} = 2.0 \pm 0.4$  and  $\omega_0(532) = 0.92 \pm 0.02$ , which differ

**Spectral aerosol optical properties by a multi-instrumental approach**

S. Segura et al.

Title Page

Abstract

Introduction

Conclusions

References

Tables

Figures

⏪

⏩

◀

▶

Back

Close

Full Screen / Esc

Printer-friendly Version

Interactive Discussion



## Spectral aerosol optical properties by a multi-instrumental approach

S. Segura et al.

Title Page

Abstract

Introduction

Conclusions

References

Tables

Figures

◀

▶

◀

▶

Back

Close

Full Screen / Esc

Printer-friendly Version

Interactive Discussion

from our values in Granada during July 2012,  $\alpha_{\text{scat},450-700} = 1.3 \pm 0.3$  and  $\omega_0(637) = 0.76 \pm 0.08$ , consistent with the prevalence of diesel traffic on the highway near the measurement site. These differences between both sites are significant and make the parameterization function of  $C(\lambda)$  given by Schmid et al. (2006) not applicable to our measurements. Therefore, based on their work, the iterative procedure has been used to calculate  $\alpha_{\text{abs}}$  and, then,  $C(\lambda)$  and  $b_{\text{abs}}(\lambda)$ , following these steps:

1. The Ångström exponent of attenuation ( $\alpha_{\text{atn}}$ ) is calculated by fitting the logarithm of the spectral attenuation coefficients with a linear fit as presented in Eq. (11).
2. The  $\alpha_{\text{atn}}$  is used in Eq. (14) as a first estimation of  $\alpha_{\text{abs}}$ , to obtain  $\omega_0(\lambda)$  and then, the compensation factor  $C$  for each Aethalometer wavelength is calculated using Eq. (12).
3. The compensation factor  $C(\lambda)$  at different wavelengths is used in Eq. (7) to obtain the new compensated absorption coefficients ( $b_{\text{abs}}$ ).
4. This new  $b_{\text{abs}}(\lambda)$  is used again in step 1 to get a better estimation for  $\alpha_{\text{abs}}$ .
5. Repeat steps 2–4 until  $\alpha_{\text{abs}}$  converges with a precision of 0.005.

## 4 Results of the compensations

### 4.1 Non-compensated/compensated Aethalometer vs. MAAP data

In Fig. 3a, non-compensated Aethalometer data ( $b_{\text{ATN}}$ ) at 637 nm obtained using Eq. (11) are compared to  $b_{\text{abs, MAAP}}$  values. The Aethalometer and the MAAP are well correlated, with  $R = 0.917$ , while the slope 3.66 shows the relationship between the Aethalometer attenuation coefficient and the MAAP absorption.

After Weingartner's compensation (Weingartner et al., 2003) is applied to the Aethalometer attenuation coefficient, we obtain the compensated Aethalometer absorption coefficient ( $b_{\text{abs, W}}$ ). The slope between  $b_{\text{abs, W}}$  and  $b_{\text{abs, MAAP}}$  changes to

## Spectral aerosol optical properties by a multi-instrumental approach

S. Segura et al.

Title Page

Abstract

Introduction

Conclusions

References

Tables

Figures

◀

▶

◀

▶

Back

Close

Full Screen / Esc

Printer-friendly Version

Interactive Discussion



1.005 and there appears a slight increase of the correlation coefficient: from 0.917 to 0.926 (Fig. 3b). The compensation factors used ( $C_{637} = 4.22 \pm 0.06$  and  $f_{637} \approx f_{660} = 1.131$ ) were already obtained in Sect. 3.2.2. Dispersion of some points is due to some noise in the data which has not been removed by the filtration algorithm described above in Sect. 3.2.1. We can further reduce this dispersion by averaging the data over a more extended period of time. Furthermore, the compensated  $b_{\text{abs}, W}$  values are on average 73 % lower than corresponding non-corrected  $b_{\text{ATN}}$  values and differ from  $b_{\text{abs}, \text{MAAP}}$  on average by around 2 %.

The statistics of the comparison between the two data sets are shown in Table 2. Average values of  $b_{\text{abs}, \text{MAAP}}$  and  $b_{\text{abs}, W}$  with their standard deviations are  $9.2 \pm 5.8 \text{ Mm}^{-1}$  and  $9.4 \pm 6.1 \text{ Mm}^{-1}$ , respectively. The 25th and 95th percentile for both data sets are very similar indicating a similar distribution of the data. The statistical analysis shows a good agreement between  $b_{\text{abs}, \text{MAAP}}$  and  $b_{\text{abs}, W}$ . Therefore it is concluded that Weingartner's compensation, with our site specific compensation parameters, compensates satisfactorily the Aethalometer  $b_{\text{ATN}}$  to obtain absorption coefficients which agree well with those measured by the MAAP.

### 4.2 Compensation parameters at different wavelengths and final compensation

The spectral dependence of  $C$  can be obtained using Eq. (12). To start,  $C^*$  and  $m_s$  as proposed in Arnott et al. (2005) for 660 nm were used (see Table 2). The  $C_{660}$  value of 2.21 was obtained, which is only  $\sim 50\%$  of the value obtained at 637 nm (see previous Sect. 3.2.2). Applying this compensation factor leads to unsatisfactory comparison with  $b_{\text{abs}, \text{MAAP}}$ , since the new compensated data is overestimating the MAAP data (slope of 1.92). The statistics of the comparison of this two data sets are shown in Table 2 as  $b_{\text{abs}, \text{Arnott}}$ . These results corroborate that the  $C^*$  and  $m_s$  parameter values from Arnott et al. (2005) are not applicable for this campaign. To get a better estimation of the spectral dependence on  $C$ , specific ambient measurements were calculated to obtain  $C^*(\lambda)$ . As we only have available  $C_{637}$  for the direct comparison

## Spectral aerosol optical properties by a multi-instrumental approach

S. Segura et al.

Title Page

Abstract

Introduction

Conclusions

References

Tables

Figures

⏪

⏩

◀

▶

Back

Close

Full Screen / Esc

Printer-friendly Version

Interactive Discussion

of the two absorption photometers,  $C_{637}^*$  can be calculated by using Eq. (12) and assuming  $m_s(637) \approx m_s(660) = 0.0713$  (Table 1). The value obtained is 3.93 which differs from the value obtained by Arnott et al. (2005) in the laboratory ( $C_{\text{Arnott}}^*$  of 2.182 at 660 nm), as can be seen in Table 1. On the other hand, this value is consistent with their proposal of  $C^*(521) = 3.69$  for ambient measurements. Following this,  $C^*(\lambda)$  values at other wavelengths have been calculated assuming the same spectral dependence of  $C_{\text{Arnott}}^*(\lambda)$  given by Arnott et al. (2005) and normalized to  $C_{\text{Arnott}}^*(660)$ . As can be seen from Table 1, the obtained  $C^*(\lambda)$  are much higher than those estimated by Arnott et al. (2005) or by Weingartner et al. (2003) in the laboratory.

Once we have retrieved the  $C^*(\lambda)$  values, the iterative method explained in Sect. 3.2.3 has been applied for each measurement to calculate the  $C(\lambda)$ , which will be used to compensate  $b_{\text{ATN}}(\lambda)$ . Almost 93% of the data converges at the fourth iteration while the remaining 7% do at the fifth iteration. The averaged values for  $C(\lambda)$  are shown in Table 1. It is evident that  $C$  increases with  $\lambda$ , from 3.42 in the UV (370 nm) channel to 4.59 in the infrared (950 nm). Comparing these values with our reference  $C_{637}$ , calculated using Eq. (9), a higher wavelength dependence is observed at lower wavelengths ( $\sim 23\%$  for  $C_{370}$ ) that at near infra-red wavelengths ( $\sim 4\%$  for  $C_{950}$ ). Weingartner et al. (2003) assumed that there was no wavelength dependence on  $C$  since the difference in their measurements between 450–660 nm was smaller than 10%. This is consistent with our data since the difference in  $C$  between 470–660 nm is  $\approx 8\%$ , and the only wavelength differing more is 370 nm (see Table 1). Furthermore, the differences in our calculated  $C$  values at each wavelength are similar to the ones reported in Schmid et al. (2006) for a  $\alpha_{\text{abs}} \approx 1$ . In addition, the average  $\alpha_{\text{abs}}$  obtained with the iterative method was found to be 1.09 with a standard deviation of around 0.25. We performed a sensitivity analysis on the effect of the compensation on the  $C$  values: a 15% change of the parameter  $f$  causes a change in the  $C$  values smaller than 1% for all wavelengths.

The obtained absorption coefficients are, on average, around a 72% and 79% lower than the corresponding  $b_{\text{ATN}}$  values measured at 370 and 950 nm, respectively. Rizzo

## Spectral aerosol optical properties by a multi-instrumental approach

S. Segura et al.

Title Page

Abstract

Introduction

Conclusions

References

Tables

Figures

◀

▶

◀

▶

Back

Close

Full Screen / Esc

Printer-friendly Version

Interactive Discussion



et al. (2011) reported a decrease of a 75 % at 450 nm, which is similar to the findings in this study. Figure 4 shows a boxplot of the compensated absorption coefficients  $b_{\text{abs}}$  at each wavelength obtained from the Aethalometer and the MAAP. On one hand, it can be seen that the MAAP absorption coefficient is in reasonable agreement with the boxes from the compensated Aethalometer data at 590 and 660 nm. This is expected when the data are properly compensated, since the spectral behavior of the absorption coefficient follows a power law as shown in Eq. (10).

Rizzo et al. (2011) performed sensitivity tests and showed that the main source of error due to  $b_{\text{abs}}$  and  $\alpha_{\text{abs}}$  is driven by the choice of  $\alpha_{\text{scat}}$ . Since they used averaged values over the whole measurement period, their sensitivity tests consisted in varying these values and see how this affected the final result for  $b_{\text{abs}}$  and  $\alpha_{\text{abs}}$ . They obtained a maximum deviation in the results of  $\pm 10\%$  and  $\pm 40\%$  on  $b_{\text{abs}}$  and  $\alpha_{\text{abs}}$ , respectively. Following their tests, in our measurements, only  $\pm 1\%$  for  $b_{\text{abs}}$  and  $\pm 2\%$  for  $\alpha_{\text{abs}}$  deviations are observed. This is due to the fact that we have used concurrent absorption and scattering measurements at multiple wavelengths and have thus reduced deviations in  $b_{\text{abs}}$  and  $\alpha_{\text{abs}}$  significantly.

## 5 Spectral absorption coefficient, spectral single scattering albedo, and Ångström exponent of absorption

### 5.1 Temporal evolution of aerosol spectral properties

The statistics obtained for  $b_{\text{abs}}(\lambda)$ , and  $\omega_0(\lambda)$  from the whole measurement campaign are shown in Table 3. For  $\alpha_{\text{abs}, 370-950}$  an average value of 1.09 is calculated with a standard deviation of 0.25. Values of  $\alpha_{\text{abs}}$  around 1 are related to the presence of traffic aerosols (Sun et al., 2007) and are typical of urban areas (Bergstrom et al., 2007). This shows a good agreement with the characteristics of the site. Maxima are greater than 1.55 (P95) and reach values up to 2.5. These high values are related to special

aerosol episodes (dust and biomass burning particles) affecting Granada during the measurement period, which will be described in more detail below.

Average values obtained for the compensated  $b_{\text{abs}}$  ranged from  $16 \text{ Mm}^{-1}$  (at 370 nm) to  $6 \text{ Mm}^{-1}$  (at 950 nm) with standard deviations of 10 and  $3 \text{ Mm}^{-1}$ , respectively. Lowest values of  $b_{\text{abs}}$  were measured at near infrared channels, 880 nm and 950 nm. In Table 3 it is obvious that for the 7 channels the difference between P25 and P95 is considerable. This is due to the fact that our site is strongly affected by traffic which generates high peaks in the absorption coefficients causing strong differences between  $b_{\text{abs}}$  at low traffic hours and rush hours (see Fig. 5d).

Finally, the statistics for  $\omega_0$  obtained for the seven Aethalometer channels were calculated. Averaged  $\omega_0$  values from 370 nm to 950 nm lie between 0.78 and 0.74, with a standard deviation of 0.08–0.09. Lyamani et al. (2010) reported an average value of  $\omega_0(670)$  of  $0.73 \pm 0.06$  in summer, which is close to the value obtained in this work,  $\omega_0(670)$  of  $0.76 \pm 0.08$ . P25 values are 0.68 and 0.74 at 950 nm and 370 nm, and P95 values are 0.88 and 0.90 at 950 nm and 370 nm, respectively. In general, the  $\omega_0(\lambda)$  average values show that during the measurement period the atmosphere in Granada at surface level contained a large fraction of absorbing particles.

Figure 5 shows the temporal evolution of hourly and daily averaged data for the different optical aerosol parameters calculated in the previous section during the period from 29 June to 29 July. Figure 5a and b display the hourly and daily average values of  $\omega_0(\lambda)$  obtained for the 370 nm and 950 nm channels of the Aethalometer. In Fig. 5a it can be observed that the  $\omega_0$  presents minima of 0.5–0.6 correspond to maximum peaks of  $b_{\text{abs}}$  (Fig. 5d). These maxima in  $b_{\text{abs}}$  are consequence of traffic emissions, this suggests that lower values of  $\omega_0$  are caused by traffic emissions which increase the absorbing component at surface level (Lyamani et al., 2010, 2011). During the whole period  $\omega_{0,950}$  is higher than  $\omega_{0,370}$ , except for ordinal days 181 (29 June) and 202–203 (20 and 21 July) (Fig. 5). A more detailed analysis of these days will be discussed below.

## Spectral aerosol optical properties by a multi-instrumental approach

S. Segura et al.

Title Page

Abstract

Introduction

Conclusions

References

Tables

Figures

⏪

⏩

◀

▶

Back

Close

Full Screen / Esc

Printer-friendly Version

Interactive Discussion







trajectories suggests that the decoupled layer extending from 2000 to 3000 m.a.s.l. was originated in North Africa. This is a clear evidence of the Saharan dust outbreak over our station.

To study whether there is any noticeable effect in the optical properties at ground level or not, the 24 h average values of both  $\omega_0(\lambda)$  and  $b_{\text{abs}}(\lambda)$  obtained on 29–30 June and 20–21 July are shown in Fig. 9a and b, respectively. Figure 9a shows a strong spectral dependence of  $\omega_0(\lambda)$  on 29 June with considerably lower values ( $\sim 0.80$ ) for the UV channel than in the IR, which is a well-known characteristic of dust. On 30 June, the spectral dependence of  $\omega_0(\lambda)$  is not strong, and can be related to fact that the dust intrusion is over and urban aerosols are dominant again. Collaud-Coen et al. (2004) proposed a method for detecting Saharan dust events based on the change of the Ångström exponent of single scattering albedo. Negative exponent values of the  $\omega_0$  ( $\alpha_{\text{SSA}}$ ) are due to the large size of mineral aerosols. In our case, on 29 June a  $\alpha_{\text{SSA}} = -0.09$  is obtained, which is related to the presence of dust in the atmosphere. On 30 June this wavelength dependence decreased to  $\alpha_{\text{SSA}} = -0.007$ , indicating that the mineral dust intrusion was over. In the case of the  $b_{\text{abs}}(\lambda)$  a stronger spectral dependence for the values obtained on 29 than for the 30 of June is found (Fig. 9b). This spectral dependence leads to the values of  $\alpha_{\text{abs}}$  of 1.34 and 1.09 on 29 and 30 June, respectively. The return of the exponent to a value close to 1 is consistent with diesel aerosols becoming predominant again. Figure 5c shows that the  $\alpha_{\text{abs}}$  reached values up to nearly 2.0 during the dust intrusion on 29 June. To study the consistency of the  $\alpha_{\text{abs}}$  values obtained during this dust event, they were compared with those obtained in other studies. Collaud-Coen et al. (2004) reported  $\alpha_{\text{abs}}$  values between 1.5 and 1.8 during Saharan dust events at Jungfraujoch, as well as a non-negligible spectral dependence of  $\omega_0$ . Values of  $\alpha_{\text{abs}}$  of 2.2 were reported by Bergstrom et al. (2002) for mixed urban pollution and desert dust aerosols in ACE Asia program. Therefore, it can be concluded that our determination of the Saharan dust episodes and the associated values of the Ångström exponent of single scattering albedo are in good agreement with the published values.

## Spectral aerosol optical properties by a multi-instrumental approach

S. Segura et al.

Title Page

Abstract

Introduction

Conclusions

References

Tables

Figures

◀

▶

◀

▶

Back

Close

Full Screen / Esc

Printer-friendly Version

Interactive Discussion







measurement period two different sources of aerosolized particulate matter affecting Granada were investigated and the differences between working days and Sundays were presented.

The attenuation coefficient at 637 nm was compensated applying the method proposed by Weingartner et al. (2003) and then compared to  $b_{\text{abs}}$  obtained from MAAP measurements. Furthermore, site specific parameters for the loading ( $R(f, \text{ATN})$ ) and multiple scattering ( $C$ ) were obtained. The values for  $f$  range from 1.15 at 370 nm to 1.11 at 950 nm, which is consistent with previous values reported by Weingartner et al. (2003), Sandradewi et al. (2008b), and Collaud-Coen et al. (2010), among others. Compensated data from both instruments were checked for any remaining loading effects and none were found.

For the multiple scattering effect, the  $C$  value at 637 nm was found to be  $4.22 \pm 0.06$  and it is in agreement with values published in the literature for sites with similar characteristics. Results of the comparison with the MAAP give a slope of 1.005 and a correlation coefficient of 0.926. Therefore, the compensated factors obtained in this study provide a satisfactory compensation of the data and are used to calculate the  $C$  factor at other wavelengths.

To obtain the wavelength dependence of  $C(\lambda)$ , the additional parameters  $m_s$  and  $C^*$  are needed, which were obtained by Arnott et al. (2005) in laboratory experiments. These values proved to be quite low when applied to ambient measurements, so new  $C^*(\lambda)$  values were calculated in this study. The  $C^*$  value for ambient data calculated at 637 nm for this campaign exhibits a value of 3.93, while  $m_s$  used is the value provided by Arnott et al. (2005). Differences in  $C^*$  agree with those expected from Arnott et al. (2005) for ambient measurements. The same spectral dependence as in Arnott et al. (2005) has been used to obtain  $C^*$  at other wavelengths.

Applying the iterative procedure proposed by Schmid et al. (2006),  $C(\lambda)$ ,  $\omega_0(\lambda)$ , and  $\alpha_{\text{abs}, 370-950}$  were calculated.  $C$  values obtained span from 3.40 at 370 nm to 4.35 at 950 nm, and their spectral differences are in agreement with the ones observed in Schmid et al. (2006) for the Amazonian Basin.

**Spectral aerosol optical properties by a multi-instrumental approach**

S. Segura et al.

Title Page

Abstract

Introduction

Conclusions

References

Tables

Figures

⏪

⏩

◀

▶

Back

Close

Full Screen / Esc

Printer-friendly Version

Interactive Discussion



## Spectral aerosol optical properties by a multi-instrumental approach

S. Segura et al.

Title Page

Abstract

Introduction

Conclusions

References

Tables

Figures

⏪

⏩

◀

▶

Back

Close

Full Screen / Esc

Printer-friendly Version

Interactive Discussion

Once the different parameters are corrected and calculated at each wavelength, a study of their temporal evolution was performed. Averaged values of  $\omega_0$  range between 0.784 (at 370 nm) and 0.737 (at 950 nm) indicating that during July 2012 Granada's atmosphere was significantly burdened with absorbing particles. This is in agreement with results obtained by Lyamani et al. (2010) for the summer period. An average value of 1 for  $\alpha_{\text{abs}}$  is explained by the fact that Granada's site is dominated by urban aerosols (Sun et al., 2007) whose major source is traffic.

Finally, the difference between working days and Sundays shows that the absorption coefficients are higher during working days than during Sundays as a consequence of the traffic intensity on the highway close to the station. These values cause decreases in  $\omega_0$  leading to an atmosphere with more absorbing particles during the working days. However,  $\alpha_{\text{abs}}$  is not affected and exhibits no differences between work days and Sundays as this value is more related to the aerosol type and their source, which does not strongly change at this site.

*Acknowledgements.* The authors gratefully acknowledge the NOAA Air Resources Laboratory (ARL) for the provision of the HYSPLIT transport and dispersion model and/or READY website used in this publication. Also, we acknowledge the Naval Research Laboratory for providing the NAAPS data in their website. This work was financed jointly by the Spanish Ministry of Economy and Competitiveness and the European Regional Development Fund through projects CGL2011-24290, CGL2010-18782, CSD2007-00067 and CGL2012-33294 by the Valencia Autonomous Government through project PROMETEO/2010/064, the Andalusia Regional Government through projects P08- RNM-3568 and P10-RNM-6299, and by the Slovenian Ministry of Economic Development and Technology JR-KROP grant 3211-11-000519. The research leading to these results has received funding from the European Union Seventh Framework Programme (FP7/2007-2013) under grant agreement Nr. 262 254 [ACTRIS]. The collaboration of S. Segura in this work was possible thanks to fellowship BES-2010-031626.

## References

- Anderson, T. L. and Ogren, J. A.: Determining aerosol radiative properties using the TSI 3563 integrating nephelometer, *Aerosol Sci. Tech.*, 29, 57–69, 1998.
- Anderson, T. L., Covert, D. S., Marshall, S. F., Laucks, M. L., Charlson, R. J., Waggoner, A. P.,  
5 Ogren, J. A., Caldow, R., Holm, R. L., Quant, F. R., Sem, G. J., Wiedensohler, A.,  
Ahlquist, N. A., and Bates, T. S.: Performance characteristics of a high sensitivity, three-  
wavelength, total scatter/backscatter nephelometer, *J. Atmos. Ocean Tech.*, 13, 967–986,  
1996.
- Ångström, A.: On the atmospheric transmission of sun radiation and on dust in the air, *Geogr.*  
10 *Ann.*, 11, 156–166, 1929.
- Arnott, W. P., Hamasha, K., Moosmuller, H., Sheridan, P. J., and Ogren, J. A.: Towards aerosol  
light-absorption measurements with a 7-wavelength aethalometer: evaluation with a photoacoustic instrument and 3-wavelength nephelometer, *Aerosol Sci. Tech.*, 39, 17–29, 2005.
- Ballach, J., Hitzengerger, R., Schultz, E., and Jaeschke, W.: Development of an improved optical transmission technique for black carbon (BC) analysis, *Atmos. Environ.*, 35, 2089–2100,  
15 2001.
- Baron, P. A. and Willeke, K.: *Aerosol Measurement: Principles, Techniques, and Applications*, John Wiley, Hoboken, NJ, 2005
- Bergstrom, R. W., Russell, P. B., and Hignett, P.: Wavelength dependence of the absorption of  
20 black carbon particles: predictions and results from the TARFOX experiment and implications  
for the aerosol single scattering albedo, *J. Atmos. Sci.*, 59, 567–577, 2002.
- Bergstrom, R. W., Pilewskie, P., Russell, P. B., Redemann, J., Bond, T. C., Quinn, P. K., and Sierau, B.: Spectral absorption properties of atmospheric aerosols, *Atmos. Chem. Phys.*, 7, 5937–5943, doi:10.5194/acp-7-5937-2007, 2007.
- 25 Boesenberg, J., Balis, D., Flamant, P., Papalardo, G., Papayanis, A., Pelon, J., Schneider, J.,  
Trickl, T., and Visconti, G.: EARLINET: a European Aerosol Research Lidar Network, *Advances in Remote Sensing, Selected Papers from the 20th International Laser Radar Conference, Vichy, France, 10–14 July 2000*, edited by: Dabas, A., Flamant, P., and Pelon, J., 155–158, 2001.
- 30 Bond, T. C. and Bergstrom: Light absorption by carbonaceous particles: an investigative review, *Aerosol Sci. Tech.*, 40, 27–67, doi:10.1080/02786820500421521, 2006.

### Spectral aerosol optical properties by a multi-instrumental approach

S. Segura et al.

Title Page

Abstract

Introduction

Conclusions

References

Tables

Figures

◀

▶

◀

▶

Back

Close

Full Screen / Esc

Printer-friendly Version

Interactive Discussion



## Spectral aerosol optical properties by a multi-instrumental approach

S. Segura et al.

Title Page

Abstract

Introduction

Conclusions

References

Tables

Figures

◀

▶

◀

▶

Back

Close

Full Screen / Esc

Printer-friendly Version

Interactive Discussion

- Bond, T. C., Anderson, T. L., and Campbell, D.: Calibration and intercomparison of filter-based measurements of visible light absorption by aerosols, *Aerosol Sci. Tech.*, 30, 582–600, 1999.
- Brito, J., Rizzo, L. V., Herckes, P., Vasconcellos, P. C., Caumo, S. E. S., Fornaro, A., Ynoue, R. Y., Artaxo, P., and Andrade, M. F.: Physical–chemical characterisation of the particulate matter inside two road tunnels in the São Paulo Metropolitan Area, *Atmos. Chem. Phys.*, 13, 12199–12213, doi:10.5194/acp-13-12199-2013, 2013.
- Chand, D., Guyon, P., Artaxo, P., Schmid, O., Frank, G. P., Rizzo, L. V., Mayol-Bracero, O. L., Gatti, L. V., and Andreae, M. O.: Optical and physical properties of aerosols in the boundary layer and free troposphere over the Amazon Basin during the biomass burning season, *Atmos. Chem. Phys.*, 6, 2911–2925, doi:10.5194/acp-6-2911-2006, 2006.
- Christensen, J. H.: The Danish Eulerian hemispheric model – a three-dimensional air pollution model used for the arctic, *Atmos. Environ.*, 31, 4169–4191, 1997.
- Collaud Coen, M., Weingartner, E., Schaub, D., Hueglin, C., Corrigan, C., Henning, S., Schwikowski, M., and Baltensperger, U.: Saharan dust events at the Jungfraujoch: detection by wavelength dependence of the single scattering albedo and first climatology analysis, *Atmos. Chem. Phys.*, 4, 2465–2480, doi:10.5194/acp-4-2465-2004, 2004.
- Collaud Coen, M., Weingartner, E., Apituley, A., Ceburnis, D., Fierz-Schmidhauser, R., Flenje, H., Henzing, J. S., Jennings, S. G., Moerman, M., Petzold, A., Schmid, O., and Baltensperger, U.: Minimizing light absorption measurement artifacts of the Aethalometer: evaluation of five correction algorithms, *Atmos. Meas. Tech.*, 3, 457–474, doi:10.5194/amt-3-457-2010, 2010.
- De Castro, B. R., Wang, L., Mihalic, J. N., Breysse, P. N., and Geyh, A. S.: The longitudinal dependence of black carbon concentration on traffic volume in an urban environment, *Japca J. Air Waste Ma.*, 58, 928–393, 2008.
- Draxler, R. R. and Rolph, G. D.: HYSPLIT (HYbrid Single-Particle Lagrangian Integrated Trajectory), available at: [www.arl.noaa.gov/ready/hysplit4.html](http://www.arl.noaa.gov/ready/hysplit4.html) (last access: November 2013), NOAA Air Resources Laboratory, Silver Spring, MD, 2003.
- Dubovik, O., Holben, B., Eck, T. F., Smirnov, A., Kaufman, Y. J., King, M. D., Tanré, D., and Slutsker, I.: Variability of absorption and optical properties of key aerosol types observed in worldwide locations, *J. Atmos. Sci.*, 59, 590–608, 2002.
- Esteve, A. R., Estellés, V., Utrillas, M. P., and Martínez-Lozano, J. A.: In-situ integrating nephelometer measurements of the scattering properties of atmospheric aerosols at an urban coastal site in western Mediterranean, *Atmos. Environ.*, 47, 43–50, 2012.

## Spectral aerosol optical properties by a multi-instrumental approach

S. Segura et al.

Title Page

Abstract

Introduction

Conclusions

References

Tables

Figures

◀

▶

◀

▶

Back

Close

Full Screen / Esc

Printer-friendly Version

Interactive Discussion

- Fialho, P., Hansen, A. D. A., and Honrath, R. E.: A new approach to decouple dust and black carbon absorption coefficients using seven-wavelength Aethalometer data, *J. Aerosol Sci.*, 36, 267–282, 2005.
- Guerrero-Rascado, J. L., Ruiz, B., and Alados-Arboledas, L.: Multispectral lidar characterization of the vertical structure of Saharan dust aerosol over southern Spain, *Atmos. Environ.*, 42, 2668–2681, 2008.
- Gundel, L. A., Dod, R. L., Rosen, H., and Novakov, T.: The relationship between optical attenuation and black carbon concentration for ambient and source particles, *Sci. Total Environ.*, 36, 197–202, 1984.
- Hansen, A. D. A.: The Aethalometer TM, available at: [8.http://mageesci.com/images/stories/docs/Aethalometer\\_book\\_2005.07.03.pdf](http://mageesci.com/images/stories/docs/Aethalometer_book_2005.07.03.pdf), Magee Scientific Company, Berkeley, California, USA, 2005.
- Hansen, A. D. A., Rosen, H., and Novakov, T.: Real-time measurement of the absorption coefficient of aerosol particles, *Appl. Optics*, 21, 3060–3062, 1982.
- Hansen, A. D. A., Rosen, H., and Novakov, T.: The aethalometer; an instrument for the real-time measurements of optical absorption by aerosol particles, *Sci. Total Environ.*, 36, 191–196, 1984.
- Heintzenberg, J., Wiedensohler, A., Tuch, T. M., Covert, D. S., Sheridan, P. J., Ogren, J. A., Gras, J., Nessler, R., Kleefeld, C., Kalivitis, N., Aaltonen, V., Wilhelm, R.-T., and Havlicek, M.: Intercomparisons and aerosol calibrations of 12 commercial integrating nephelometers of three manufacturers, *J. Atmos. Ocean Tech.*, 23, 902–914, 2006.
- Hogan, T. F. and Brody, L. R.: Sensitivity studies of the Navy global forecast model parameterizations and evaluation of improvements to NOGAPS, *Mon. Weather Rev.*, 121, 2373–2395, 1993.
- Horvath, H.: Atmospheric light absorption: a review, *Atmos. Environ.*, 27, 293–317, 1993.
- Houghton, J. T., Ding, Y., Griggs, D. J., Noguera, M., van der Linden, P. J., and Xiaosu, D.: *Climate Change 2001: The Scientific Basis*, Cambridge Univ. Press, New York, 2001.
- Hyvärinen, A.-P., Vakkari, V., Laakso, L., Hooda, R. K., Sharma, V. P., Panwar, T. S., Beukes, J. P., van Zyl, P. G., Josipovic, M., Garland, R. M., Andreae, M. O., Pöschl, U., and Petzold, A.: Correction for a measurement artifact of the Multi-Angle Absorption Photometer (MAAP) at high black carbon mass concentration levels, *Atmos. Meas. Tech.*, 6, 81–90, doi:10.5194/amt-6-81-2013, 2013.

**Spectral aerosol optical properties by a multi-instrumental approach**

S. Segura et al.

Title Page

Abstract

Introduction

Conclusions

References

Tables

Figures

◀

▶

◀

▶

Back

Close

Full Screen / Esc

Printer-friendly Version

Interactive Discussion

IPCC: Climate Change 2013: The Physical Science Basis, Working Group I Contribution to the IPCC 5th Assessment Report – Changes to the Underlying Scientific/Technical Assessment, edited by: Stocker, T. F., Qin, D., Plattner, G.-K., Tignor, M., Allen, S. K., Boschung, J., Nauels, A., Xia, Y., Bex, V., and Midgley, P. M., Cambridge University Press, Cambridge, UK and New York, USA, 2013.

Jacobson, M. Z.: Studying the effects of aerosol son vertical photolysis rate coefficient and temperature profiles over an urban air shed, *J. Geophys. Res.*, 103, 10593–10604, 1998.

Kanaya, Y., Komazaki, Y., Pochanart, P., Liu, Y., Akimoto, H., Gao, J., Wang, T., and Wang, Z.: Mass concentrations of black carbon measured by four instruments in the middle of Central East China in June 2006, *Atmos. Chem. Phys.*, 8, 7637–7649, doi:10.5194/acp-8-7637-2008, 2008.

Kirchstetter, T. W., Novakov, T., and Hobbs, P. V.: Evidence that the spectral dependence of light absorption by aerosols is affected by organic carbon, *J. Geophys. Res.*, 109, D21208, doi:10.1029/2004JD004999, 2004.

Lack, D. A., Cappa, C. D., Cross, E. S., Massoli, P., Ahern, A. T., Davidovits, P., and Onasch, T. B.: Absorption enhancement of coated absorbing aerosols: validation of the photo-acoustic technique for measuring the enhancement, *Aerosol Sci. Tech.*, 43, 1006–1012, doi:10.1080/02786820903117932, 2009.

Lyamani, H., Olmo, F. J., and Alados-Arboledas, L.: Light scattering and absorption properties of aerosol particles in the urban environment of Granada, Spain, *Atmos. Environ.*, 42, 2630–2642, doi:10.1016/j.atmosenv.2007.10.070, 2008.

Lyamani, H., Olmo, F. J., and Alados-Arboledas, L.: Physical and optical properties of aerosols over an urban location in Spain: seasonal and diurnal variability, *Atmos. Chem. Phys.*, 10, 239–254, doi:10.5194/acp-10-239-2010, 2010.

Lyamani, H., Olmo, F. J., Foyo, I., and Alados-Arboledas, L.: Black carbon aerosols over an urban area in south-eastern Spain: changes detected after the 2008 economic crisis, *Atmos. Environ.*, 45, 6423–6432, 2011.

Moosmüller, H., Chakrabarty, R. K., and Arnott, W. P.: Aerosol light absorption and its measurement: a review, *J. Quant. Spectrosc. Ra.*, 110, 844–878, doi:10.1016/j.jqsrt.2009.02.035, 2009.

Mukai, H. and Ambe, Y.: characterization of a humic acid-like Brown substance in airborne particulate matter and tentative identification of its origin, *Atmos. Environ.*, 20, 813–819, 1986.

**Spectral aerosol optical properties by a multi-instrumental approach**

S. Segura et al.

Title Page

Abstract

Introduction

Conclusions

References

Tables

Figures

◀

▶

◀

▶

Back

Close

Full Screen / Esc

Printer-friendly Version

Interactive Discussion



- Müller, T., Henzing, J. S., de Leeuw, G., Wiedensohler, A., Alastuey, A., Angelov, H., Bizjak, M., Collaud Coen, M., Engström, J. E., Gruening, C., Hillamo, R., Hoffer, A., Imre, K., Ivanow, P., Jennings, G., Sun, J. Y., Kalivitis, N., Karlsson, H., Komppula, M., Laj, P., Li, S.-M., Lunder, C., Marinoni, A., Martins dos Santos, S., Moerman, M., Nowak, A., Ogren, J. A., Petzold, A., Pichon, J. M., Rodriguez, S., Sharma, S., Sheridan, P. J., Teinilä, K., Tuch, T., Viana, M., Virkkula, A., Weingartner, E., Wilhelm, R., and Wang, Y. Q.: Characterization and intercomparison of aerosol absorption photometers: result of two intercomparison workshops, *Atmos. Meas. Tech.*, 4, 245–268, doi:10.5194/amt-4-245-2011, 2011.
- Nakayama, T., Kondo, Y., Moteki, N., Sahu, L. K., Kinase, T., Kita, K., and Matsumi, Y.: Size-dependent correction factors for absorption measurements using filter-based photometers: PSAP and COSMOS, *J. Aerosol Sci.*, 41, 333–343, 2010.
- Park, S. S., Hansen, A. D. A., and Cho, Y.: Measurement of real time black carbon for investigating spot loading effects of Aethalometer data, *Atmos. Environ.*, 11, 1449–1455, 2010.
- Petzold, A. and Schonlinner, M.: Multi-angle absorption photometry – a new method for the measurement of aerosol light absorption and atmospheric black carbon, *J. Aerosol Sci.*, 35, 421–441, 2004.
- Petzold, A., Kopp, C., and Niessner, R.: The dependence of the specific attenuation cross section on black carbon mass fraction and particle size, *Atmos. Environ.*, 31, 661–672, 1997.
- Petzold, A., Schloesser, H., Sheridan, P. J., Arnott, W., Ogren, J. A., and Virkkula, A.: Evaluation of multiangle absorption photometry for measuring aerosol light absorption, *Aerosol Sci. Tech.*, 39, 40–51, 2005.
- Ramanathan, V., Crutzen, P. J., Kiehl, J. T., and Rosenfeld, D.: Aerosols, Climate, and hydrological cycle, *Science*, 7, 2119–2124, 2001.
- Rizzo, L. V., Correia, A. L., Artaxo, P., Procópio, A. S., and Andreae, M. O.: Spectral dependence of aerosol light absorption over the Amazon Basin, *Atmos. Chem. Phys.*, 11, 8899–8912, doi:10.5194/acp-11-8899-2011, 2011.
- Sandradewi, J., Prevot, A. S. H., Szidat, S., Perron, N., Lanz, V. A., Weingartner, E., and Baltensperger, U.: Using aerosol light absorption measurements for the quantitative determination of wood burning and traffic emission contributions to particulate matter, *Environ. Sci. Technol.*, 42, 3316–3323, 2008a.
- Sandradewi, J., Prevot, A. S. H., Weingartner, E., Schmidhauser, R., Gysel, M., and Baltensperger, U.: A study of wood burning and traffic aerosols in an Alpine valley using a multi-wavelength aethalometer, *Atmos. Environ.*, 42, 101–112, 2008b.

## Spectral aerosol optical properties by a multi-instrumental approach

S. Segura et al.

Title Page

Abstract

Introduction

Conclusions

References

Tables

Figures

⏪

⏩

◀

▶

Back

Close

Full Screen / Esc

Printer-friendly Version

Interactive Discussion

- Schmid, O., Artaxo, P., Arnott, W. P., Chand, D., Gatti, L. V., Frank, G. P., Hoffer, A., Schnaiter, M., and Andreae, M. O.: Spectral light absorption by ambient aerosols influenced by biomass burning in the Amazon Basin. I: Comparison and field calibration of absorption measurement techniques, *Atmos. Chem. Phys.*, 6, 3443–3462, doi:10.5194/acp-6-3443-2006, 2006.
- Sheridan, P. J., Arnott, W. P., Ogren, J. A., Andrews, E., Atkinson, D. B., Covert, D. S., Moosmuller, H., Petzold, A., Schmid, B., Strawa, A. W., Varma, R., and Virkkula, A.: The Reno Aerosol Optics Study: an evaluation of aerosol absorption measurement methods, *Aerosol Sci. Tech.*, 39, 1–16, 2005.
- Sun, H., Biedermann, L., and Bond, T. C.: Color of brown carbon: a model for ultraviolet and visible light absorption by organic carbon aerosol, *Geophys. Res. Lett.*, 34, L17813, doi:10.1029/2007GL029797, 2007.
- Titos, G., Foyo-Moreno, I., Lyamani, H., Querol, X., Alastuey, A., and Alados-Arboledas, L.: Optical properties and chemical composition of aerosol particles at an urban location: an estimation of the aerosol mass scattering and absorption efficiencies, *J. Geophys. Res.*, 117, D04206, doi:10.1029/2011JD016671, 2012.
- Virkkula, A., Makel, T., Yli-Tuomi, T., Hirsikko, A., Koponen, I. K., Hameri, K., and Hillamo, R.: A simple procedure for correcting loading effects of aethalometer data, *Japca J. Air Waste Ma.*, 57, 1214–1222, doi:10.3155/1047-3289.57.10.1214, 2007.
- Weingartner, E., Saathoff, H., Schnaiter, M., Streit, N., Bitnar, B., and Baltensperger, U.: Absorption of light by soot particles: determination of the absorption coefficient by means of aethalometers, *J. Aerosol Sci.*, 34, 1445–1463, 2003.

## Spectral aerosol optical properties by a multi-instrumental approach

S. Segura et al.

Title Page

Abstract

Introduction

Conclusions

References

Tables

Figures

◀

▶

◀

▶

Back

Close

Full Screen / Esc

Printer-friendly Version

Interactive Discussion

**Table 1.** Compensation factors obtained for the 7 Aethalometer wavelengths:  $f$  corresponds to the “shadowing effect” in the loading compensation;  $100\alpha$  is the value given in Arnott et al. (2005) to the scattering fraction of particles ( $m_s$  in Schmid et al., 2006);  $M$  is the value given in Arnott et al. (2005) to the multiple scattering compensation factor ( $C^*$  in Schmid et al. (2006) and in this work);  $C^*$  and  $C$  are the values specifically site-calculated in this work.

	Spectral compensation factors						
$\lambda$ (nm)	370	470	520	590	660	880	950
$f$	1.204	1.141	1.120	1.093	1.084	1.044	1.041
$100m_s$	3.35	4.57	5.23	6.16	7.13	10.38	11.48
$C_{\text{Arnott}}^*$	1.813	2.073	2.076	2.104	2.182	2.226	2.199
$C^*$	3.26	3.72	3.73	3.78	3.92	3.99	3.95
$C$	3.39	3.87	3.90	3.98	4.19	4.35	4.35



## Spectral aerosol optical properties by a multi-instrumental approach

S. Segura et al.

[Title Page](#)
[Abstract](#)
[Introduction](#)
[Conclusions](#)
[References](#)
[Tables](#)
[Figures](#)
[⏪](#)
[⏩](#)
[◀](#)
[▶](#)
[Back](#)
[Close](#)
[Full Screen / Esc](#)
[Printer-friendly Version](#)
[Interactive Discussion](#)

**Table 3.** Statistics of data for  $\alpha_{\text{abs}}$ ,  $\omega_0(\lambda)$ , and  $b_{\text{abs}}(\lambda)$ : mean, standard deviation, median, 25th percentile (P25), and 95th percentile (P95).

	Mean	SD	Median	Minimum	Maximum	P25	P95
$\alpha_{\text{abs}, 370-950}$	1.1	0.3	1.1	0.19	2.56	0.95	1.55
$b_{\text{abs}, 370} \text{ (Mm}^{-1}\text{)}$	16	10	14	2.9	87.0	9.3	35.9
$b_{\text{abs}, 470} \text{ (Mm}^{-1}\text{)}$	12	7	10	2.1	59.3	6.7	25.8
$b_{\text{abs}, 520} \text{ (Mm}^{-1}\text{)}$	10	6	9	1.9	50.6	5.8	22.6
$b_{\text{abs}, 590} \text{ (Mm}^{-1}\text{)}$	9	6	8	1.5	45.3	5.2	20.4
$b_{\text{abs}, 660} \text{ (Mm}^{-1}\text{)}$	8	5	7	1.4	39.5	4.5	17.9
$b_{\text{abs}, 880} \text{ (Mm}^{-1}\text{)}$	6	4	5	0.9	28.6	3.2	13.2
$b_{\text{abs}, 950} \text{ (Mm}^{-1}\text{)}$	5	3	4	0.9	26.3	2.9	12.6
$\omega_{0,370}$	0.8	0.08	0.8	0.42	0.96	0.74	0.90
$\omega_{0,470}$	0.8	0.08	0.8	0.41	0.96	0.73	0.88
$\omega_{0,520}$	0.8	0.08	0.8	0.40	0.96	0.72	0.88
$\omega_{0,590}$	0.8	0.08	0.8	0.39	0.95	0.72	0.88
$\omega_{0,660}$	0.8	0.08	0.8	0.38	0.96	0.71	0.88
$\omega_{0,880}$	0.7	0.09	0.8	0.35	0.97	0.69	0.88
$\omega_{0,950}$	0.7	0.09	0.7	0.33	0.98	0.68	0.88

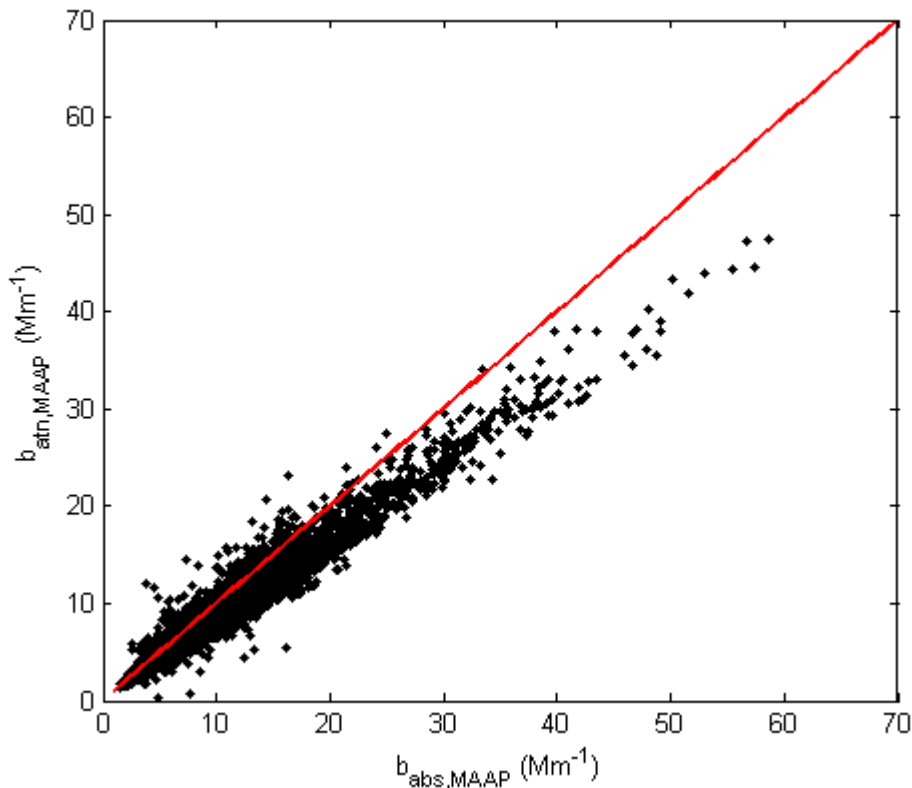


**Fig. 1.** Non-compensated absorption coefficient ( $b_{\text{atn,MAAP}}$ ) vs. compensated absorption coefficient obtained from the reflected signal ( $b_{\text{abs,MAAP}}$ ). Shows the relationship between the  $b_{\text{atn,MAAP}}$  given by the MAAP, as explained in Sect. 2.2, and the corrected  $b_{\text{abs,MAAP}}$  obtained with the reflected signal at  $165^\circ$ .

**Spectral aerosol optical properties by a multi-instrumental approach**

S. Segura et al.

Title Page	
Abstract	Introduction
Conclusions	References
Tables	Figures
◀	▶
◀	▶
Back	Close
Full Screen / Esc	
Printer-friendly Version	
Interactive Discussion	



## Spectral aerosol optical properties by a multi-instrumental approach

S. Segura et al.

Title Page

Abstract

Introduction

Conclusions

References

Tables

Figures



Back

Close

Full Screen / Esc

Printer-friendly Version

Interactive Discussion

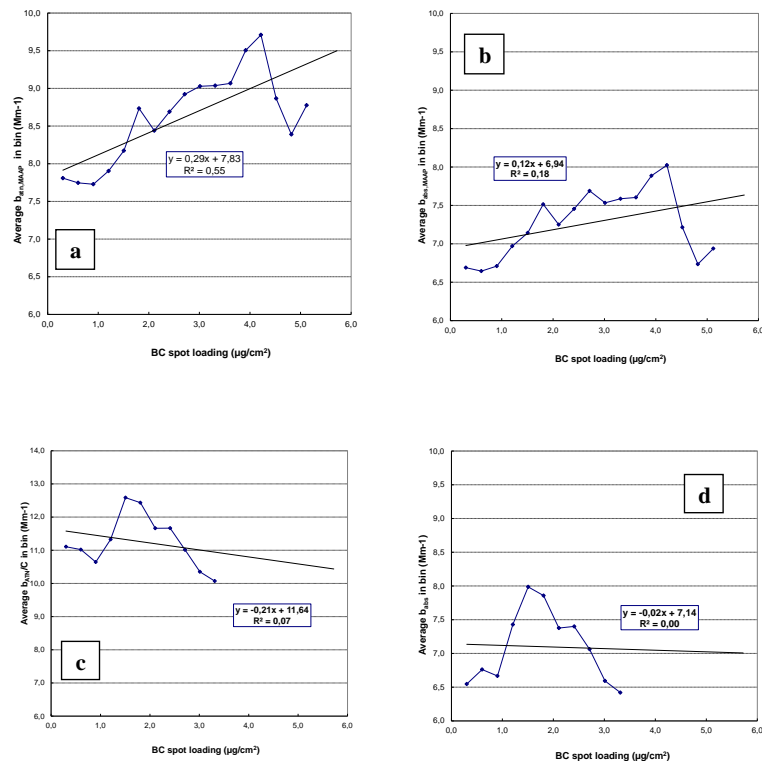


**Fig. 2.** Average attenuation or absorption coefficient vs. loading of the spot: **(a)** the non-compensated MAAP absorption coefficient  $b_{\text{abs,BC-MAAP}}$ ; **(b)** the compensated, Eq. (4), MAAP absorption coefficient  $b_{\text{abs,MAAP}}$ ; **(c)** the Aethalometer attenuation coefficient  $b_{\text{ATN,C}}$ ; **(d)** the compensated, Eq. (7), Aethalometer absorption coefficient  $b_{\text{abs}}$ . We see that the compensation of both instrumental data considerably reduces the slope for MAAP and eliminates it for the Aethalometer. It also reduces the intercept. Note the different scales.

## Spectral aerosol optical properties by a multi-instrumental approach

S. Segura et al.

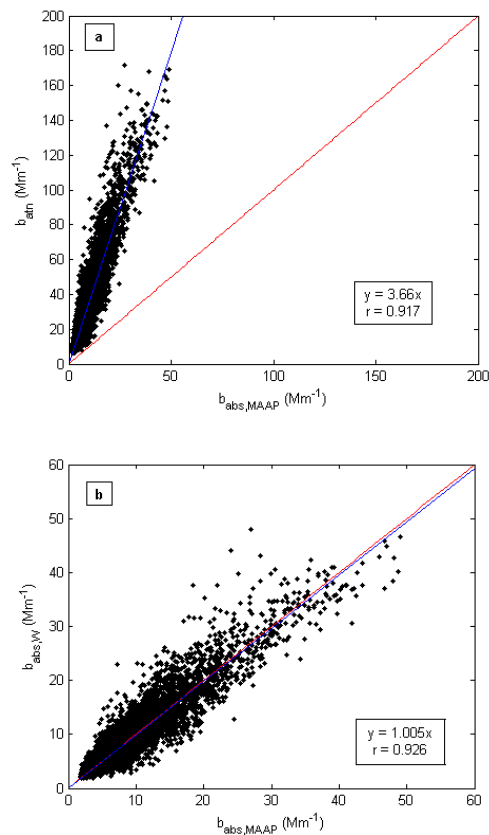


**Fig. 3.** Comparison of the Aethalometer vs. MAAP absorption coefficient ( $b_{\text{abs,MAAP}}$ ) at 637 nm for: **(a)** non-corrected Aethalometer data ( $b_{\text{ATN}}$ ) **(b)** Weingartner's compensation ( $b_{\text{abs,W}}$ ).

[Title Page](#)[Abstract](#)[Introduction](#)[Conclusions](#)[References](#)[Tables](#)[Figures](#)[⏪](#)[⏩](#)[⏴](#)[⏵](#)[Back](#)[Close](#)[Full Screen / Esc](#)[Printer-friendly Version](#)[Interactive Discussion](#)

## Spectral aerosol optical properties by a multi-instrumental approach

S. Segura et al.

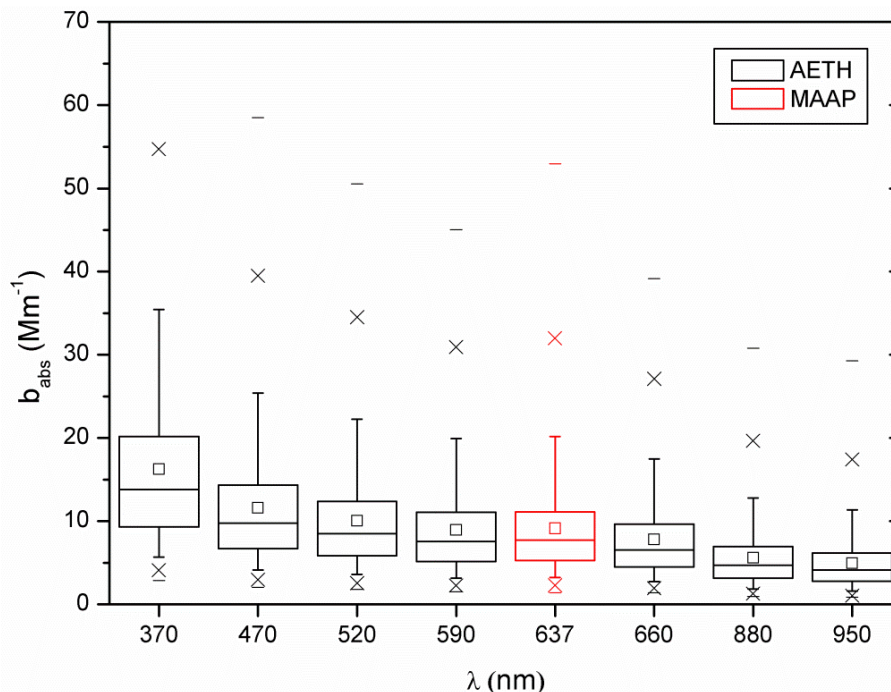


**Fig. 4.** Boxplot of the Aethalometer (black) and MAAP (red) corrected absorption coefficients ( $b_{\text{abs}}$ ). The square inside the boxes represents the average; the central line corresponds to the median; the edges of the box are the 25th and 75th percentiles; the whiskers correspond to 5th and 95th percentiles; and horizontal lines outside the boxes, maxima and minima.

## Spectral aerosol optical properties by a multi-instrumental approach

S. Segura et al.

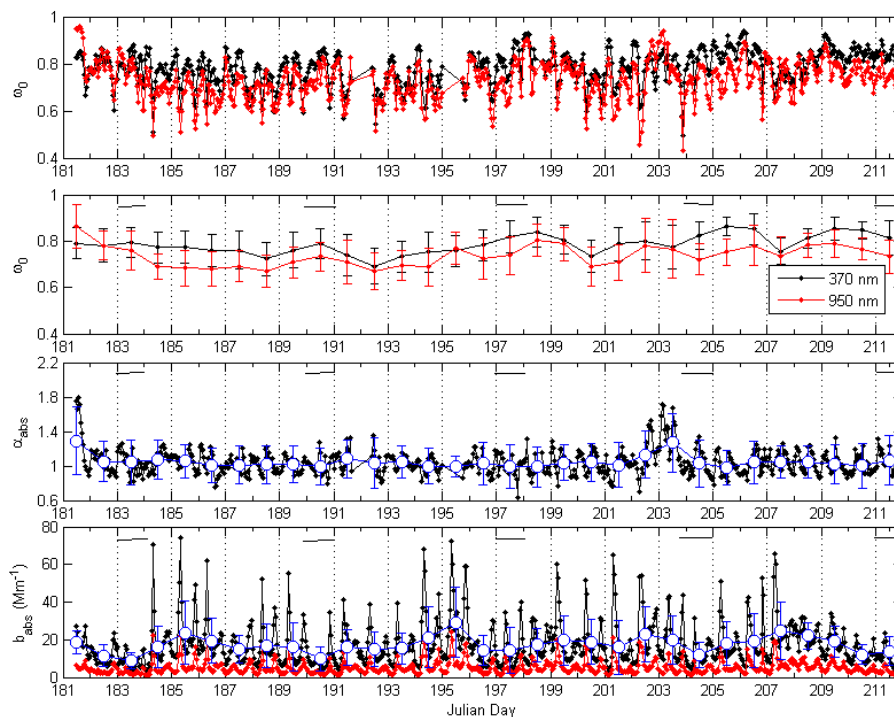


**Fig. 5.** Temporal evolution of: **(a)**  $\omega_{0,370}$  and  $\omega_{0,950}$  hourly averaged, **(b)**  $\omega_{0,370}$  and  $\omega_{0,950}$  daily averaged, **(c)**  $\alpha_{\text{abs}}$  hourly (black line) and daily averaged (blue dots), and **(d)**  $b_{\text{abs},370}$  and  $b_{\text{abs},950}$  hourly averaged, and daily averaged values for  $b_{\text{abs},370}$  (blue dots) with their standard deviations. Except for  $\alpha_{\text{abs}}$ , black lines correspond to hourly averages at 370 nm and red lines to hourly averages at 950 nm. All these data correspond to the period June–July 2012.

## Spectral aerosol optical properties by a multi-instrumental approach

S. Segura et al.

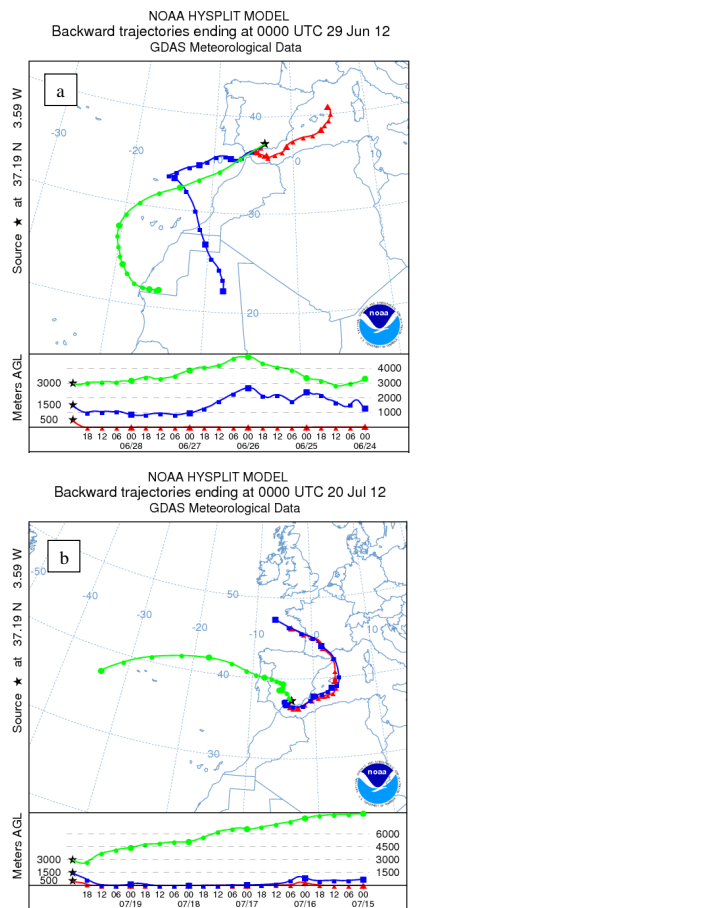


**Fig. 6.** 5 day back trajectories from HYSPLIT at three different heights (500 (red), 1500 (blue), and 3000 m a.g.l. (green)) for: **(a)** 29 June and **(b)** 20 July.

## Spectral aerosol optical properties by a multi-instrumental approach

S. Segura et al.

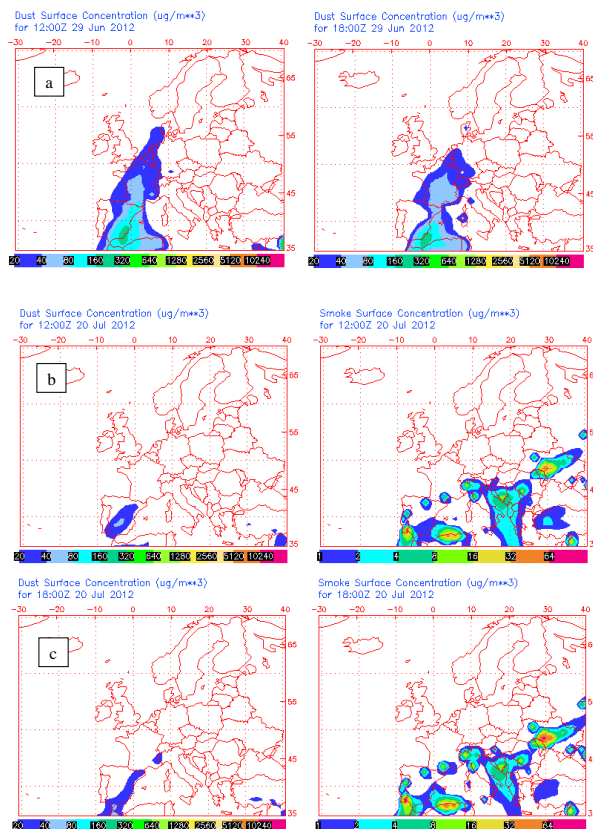


**Fig. 7.** Total surface dust and biomass burning concentration predicted by NAAPS model for the **(a)** 29 June at 12:00 UTC and 18:00 UTC, **(b)** 20 July 12:00 UTC, and **(c)** 20 July 18:00 UTC. Biomass burning concentration is only shown for the 20 July since on the 29 June there were no concentrations of this type over Granada.

[Title Page](#)[Abstract](#)[Introduction](#)[Conclusions](#)[References](#)[Tables](#)[Figures](#)[◀](#)[▶](#)[◀](#)[▶](#)[Back](#)[Close](#)[Full Screen / Esc](#)[Printer-friendly Version](#)[Interactive Discussion](#)

## Spectral aerosol optical properties by a multi-instrumental approach

S. Segura et al.

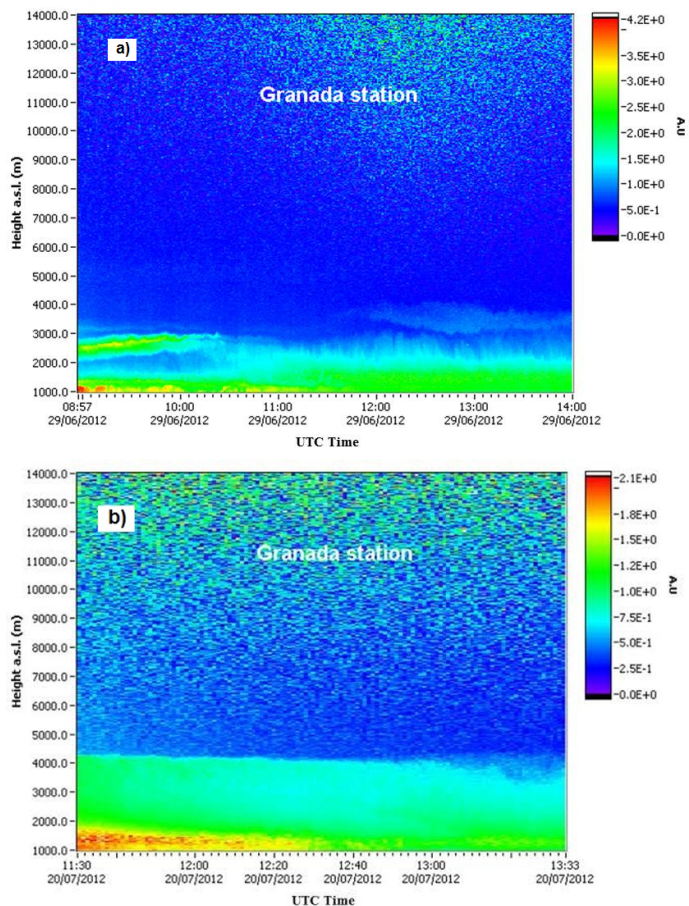


**Fig. 8.** LIDAR vertical profiles obtained for: **(a)** 29 June from 08:57 to 14:00 UTC and **(b)** 20 July 11:30 to 13:30 UTC.

[Title Page](#)[Abstract](#)[Introduction](#)[Conclusions](#)[References](#)[Tables](#)[Figures](#)[⏪](#)[⏩](#)[◀](#)[▶](#)[Back](#)[Close](#)[Full Screen / Esc](#)[Printer-friendly Version](#)[Interactive Discussion](#)

## Spectral aerosol optical properties by a multi-instrumental approach

S. Segura et al.

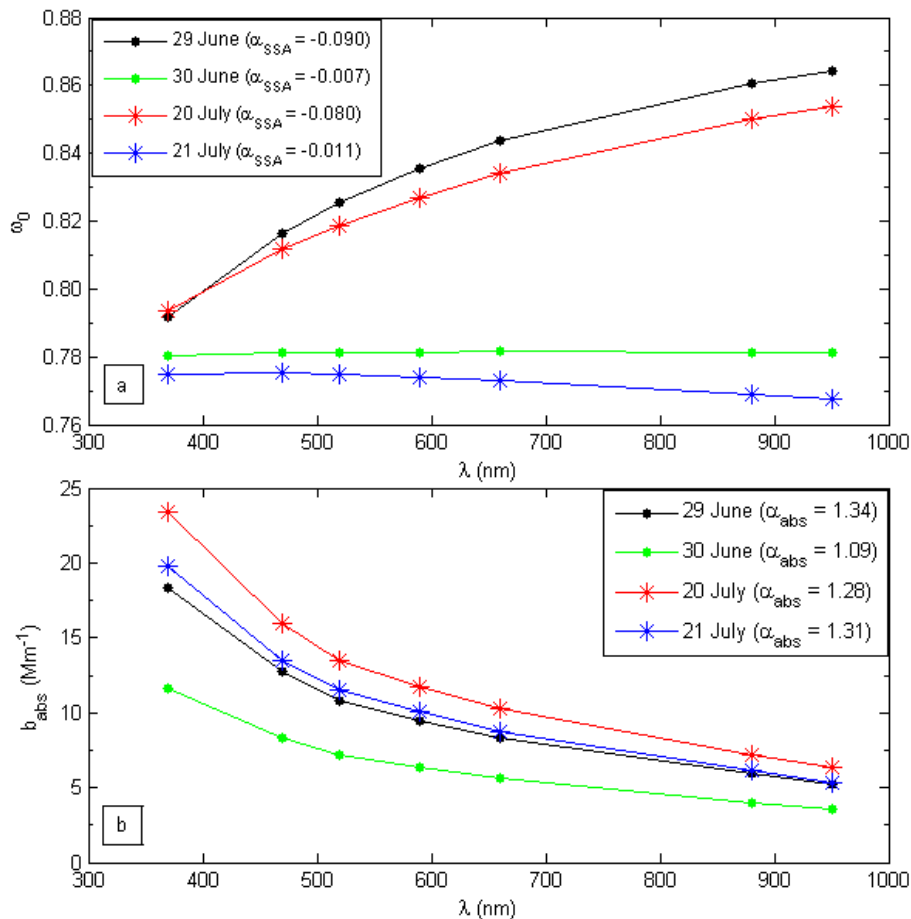


**Fig. 9.** Spectral dependence of daily averaged  $\omega_0$  and  $b_{\text{abs}}$  for the 29 June (black), 30 June (green), 20 July (red), and 21 July (blue).

## Spectral aerosol optical properties by a multi-instrumental approach

S. Segura et al.

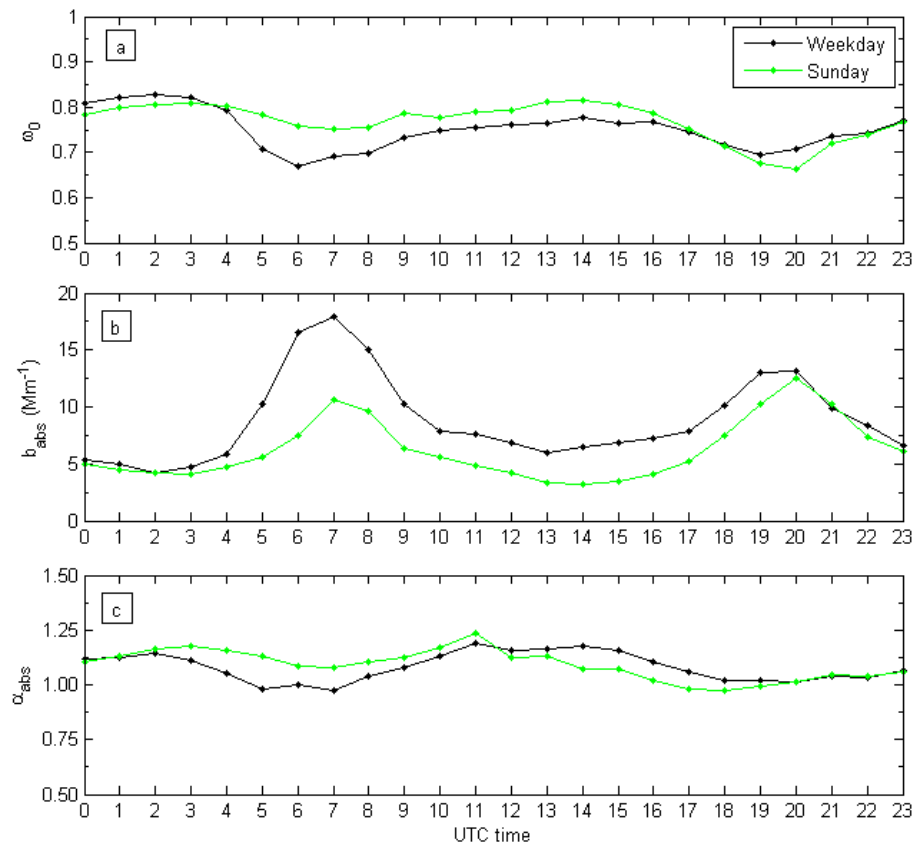


**Fig. 10.** Comparison of average during cycles for working days (black) and Sundays (green) of: **(a)** single scattering albedo ( $\omega_{0,660}$ ), **(b)** absorption coefficient ( $b_{abs,660}$ ), and **(c)**  $\alpha_{abs}$ .

Title Page

Abstract Introduction

Conclusions References

Tables Figures

◀ ▶

◀ ▶

Back Close

Full Screen / Esc

Printer-friendly Version

Interactive Discussion